Silicon nanowire arrays coupled with cobalt phosphide spheres as low-cost photocathodes for efficient solar hydrogen evolution

Xiao-Qing Bao,[a] M. Fatima Cerqueira,[b] Pedro Alpuim[ab] and Lifeng Liu*[a]

We demonstrate the first example of silicon nanowire array photocathodes coupled with hollow spheres of the emerging earth-abundant cobalt phosphide catalysts. Compared to bare silicon nanowire arrays, the hybrid electrodes exhibit significantly improved photoelectrochemical performance toward the solar-driven H_2 evolution reaction.

Silicon (Si) has long been considered a good candidate material for photoelectrochemical (PEC) water splitting to produce hydrogen (H_2).[1] In particular, remarkable progress has been made in recent years toward the fabrication of vertically aligned Si micro-/nano-wire (SiMW/SiNW) arrays, which can not only significantly improve the light absorption capability[2] and increase the electrode/electrolyte contact area, but more importantly can decouple the light propagation and charge carrier collection thereby rendering enhanced PEC performance.[3] To date, various SiMW/SiNW arrays fabricated by different methods such as reactive ion etching,[4] chemical vapor deposition (CVD),[5] and metal-assisted chemical etching (MACE)[6] have been investigated for use as photocathodes to catalyze hydrogen evolution reaction (HER). It is widely documented that bare Si has sluggish kinetics toward HER and usually generates only a small photocurrent at 0 V versus reversible hydrogen electrode (RHE) where hydrogen starts to thermodynamically evolve.[4–6] Hence, a co-catalyst, in most cases, is needed to improve the HER performance of the electrode. Platinum (Pt) is by far the most efficient and commonly used co-catalyst with SiMW/SiNW photocathodes. However, it is not practical and economically viable to use Pt on a large scale because of its high cost and scarcity. For solar H_2 fuel to be economically competitive, a non-precious, earth-abundant HER co-catalyst must be utilized. To this end, research efforts have been devoted to combining SiMW/SiNW arrays with state-of-

the-art earth-abundant HER catalysts such as molybdenum sulfide,[4,6a,6c] and PEC performance comparable to that of SiNW/Pt has been reported.

In this communication, we report the first example of photocathodes composed of SiNW arrays coupled with hollow spheres of cobalt phosphide (SiNW/Co-P), an emerging efficient earth abundant HER catalyst that was reported very recently.[7] Compared with bare SiNW arrays, the as-fabricated SiNW/Co-P photocathodes exhibit remarkable positively shifted onset potential (Vonset, defined as the potential where the cathodic current density is 1 mA cm^{-2}) for HER and greatly increased photocurrent density at 0 V vs. RHE. Furthermore, the PEC performance of SiNW/Co-P is comparable to that of SiNW arrays decorated with electrolessly deposited Pt nanoparticles (SiNW/PtNPs, see Experimental section, ESI†).[6b]

Fig. 1a schematically illustrates the fabrication process of the SiNW/Co-P photocathodes. Firstly, vertically aligned SiNWs were fabricated by MACE of a p-Si(100) wafer in a mixture of hydrofluoric acid and hydrogen peroxide for 1 min, as reported previously.[6b] This resulted in the formation of a SiNW array aligned perpendicular to the Si substrate having a wire length of ca. 2 μm (Fig. 1b). The metallic Co was then deposited on the SiNW array surface by a simple photo-assisted galvanostatic electrodeposition process (Experimental section, ESI†), considering that the photo-generated electrons at the SiNW surface would facilitate the reduction of Co^{2+} in the electrolyte.[6a] Nevertheless, it was found that Co^{2+} is mainly reduced at the top surface of the array in the form of nanoparticles, as displayed in the scanning electron microscopy (SEM) image in Fig. 1c, possibly due to the mass transfer limit of the electrolyte toward the side wall of the SiNWs. The size of the deposited Co NPs ranges from 50 to 100 nm. The Co-NP-coated SiNW array was subsequently subjected to a phosphorization treatment in a tube furnace at a fixed temperature (e.g., 400, 500 or 600 ºC), using red phosphorous as the precursor (hereafter denoted as SiNW/Co-P-400, SiNW/Co-P-500, and SiNW/Co-P-600, respectively). Fig. 1d shows a representative SEM image of the SiNW/Co-P-500 electrode where it is clearly seen that after phosphorization, the size of the topmost NPs substantially increases, amounting to 300–400 nm in diameter. Moreover, most of these Co-P NPs exhibit a more regular spherical shape.

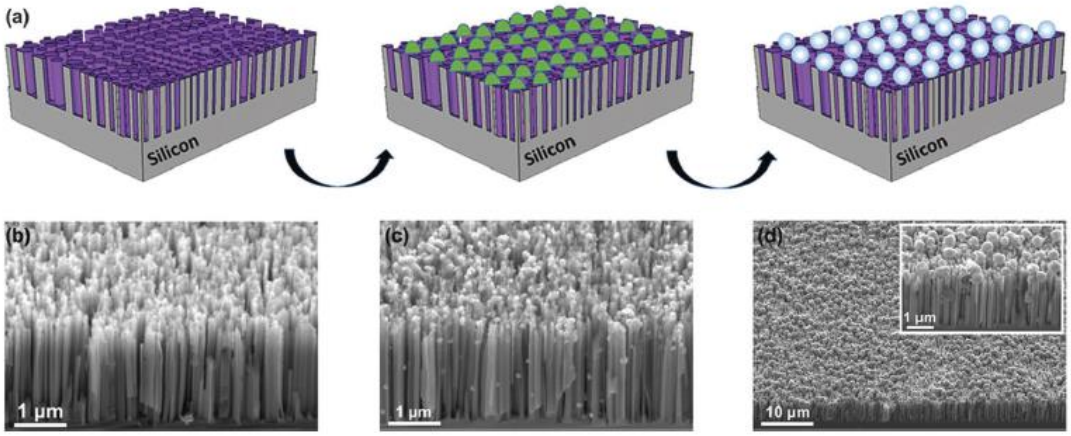

Fig 1- (a) Schematic illustration of the fabrication of Co-P sphere decorated SiNW arrays. Representative SEM micrographs of (b) the as-obtained SiNW arrays; (c) SiNW arrays coupled with photo-electrodeposited Co NPs, and (d) SiNW/Co-P-500 prepared by a phosphorization treatment at 500 ºC for 6 h in high-purity N_2.

To investigate the phase composition of the obtained Co-P NPs, X-ray diffraction (XRD) measurements were conducted.

Fig. 2 shows the XRD pattern of the SiNW/Co-P-500 electrode, from which one can see that all the diffraction peaks can be well assigned to orthorhombic Co_2P (ICDD No. 32-0306) except those located at 33.31^o, 38.31^o and 79.11^o that arise from the diffractions of the SiNWs underneath. Moreover, XRD examination indicates that phosphorization at 400 ºC results in the formation of poorly-crystallized Co_2P; while phosphorizing SiNW/CoNPs at 600 ºC gives rise to a Co-P mixture with CoP (ICDD No. 29-0497) as the major phase (Fig. S1, ESI†).

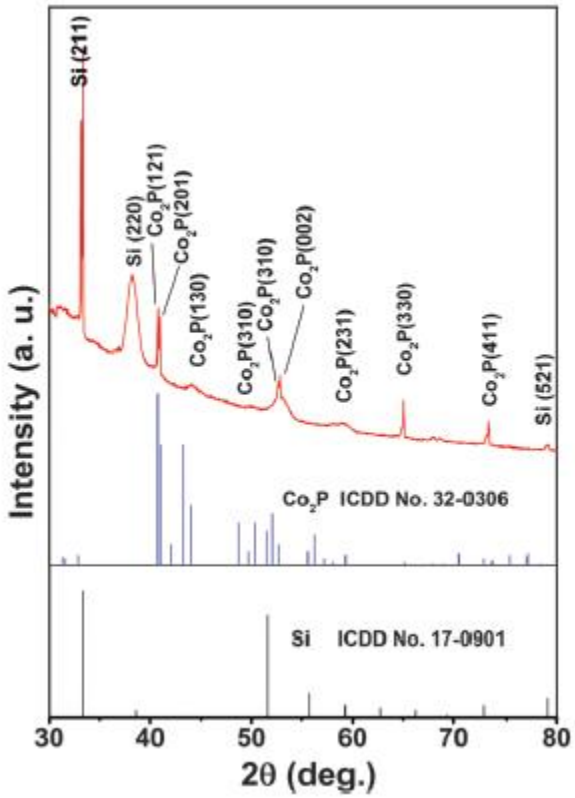

Fig 2- XRD pattern of the SiNW/Co-P-500 electrode. The standard powder XRD patterns of Si and orthorhombic Co_2P are given for reference.

To get further insight into the microstructure, the Co2P NPs were scratched off from the Si substrate and characterized by transmission electron microscopy (TEM). According to the low and high-magnification TEM micrographs, these NPs are in fact hollow spheres either with or without a core inside (Fig. 3a and b). Transformation from solid Co NPs into hollow Co_2P spheres may result from the Kirkendall effect during the phosphorization treatment, similar to that reported previously.[7b] Extensive TEM investigation reveals that the walls of Co_2P hollow spheres consist of many crystallites covered with a thin amorphous layer at the outer surface. Fig. 3c is a representative high-resolution TEM image of a Co_2P crystallite, showing well-defined single crystalline nature, as revealed in the electron diffraction (ED) pattern in the inset. The measured inter-planar spacing of the two major crystal planes is 0.331 and 0.271 nm, respectively, corresponding to that of (020) and (111) planes of orthorhombic Co_2P (ICDD No. 32-0306). The measured angle between these two planes is 65.71, in good agreement with that calculated according to the lattice parameters of the orthorhombic Co_2P. The lattice structure of the SiNWs was also investigated which confirmed their single-crystalline nature (Fig. S2, ESI†). This is consistent with previous reports on the MACE-derived SiNWs.[6d] The composition of the hollow spheres was analyzed by an

extensive energy dispersive X-ray (EDX) investigation which showed that the spheres consist exclusively of Co and P with an atomic ratio close to 5 : 3 (Fig. S3, ESI†). The excess P may originate from the condensation of P vapor on the sphere surface when cooling the sample after phosphorization. Fig. 3d and e show the high-angle annular dark-field (HAADF) STEM images of the SiNW/Co-P-500, where it is seen that the spheres are intimately attached to the SiNW bundles even after the TEM specimen preparation process using ultrasonication. Fig. 3f–h show the elemental maps of Si, Co, and P, further corroborating that the hollow spheres consist of Co and P.

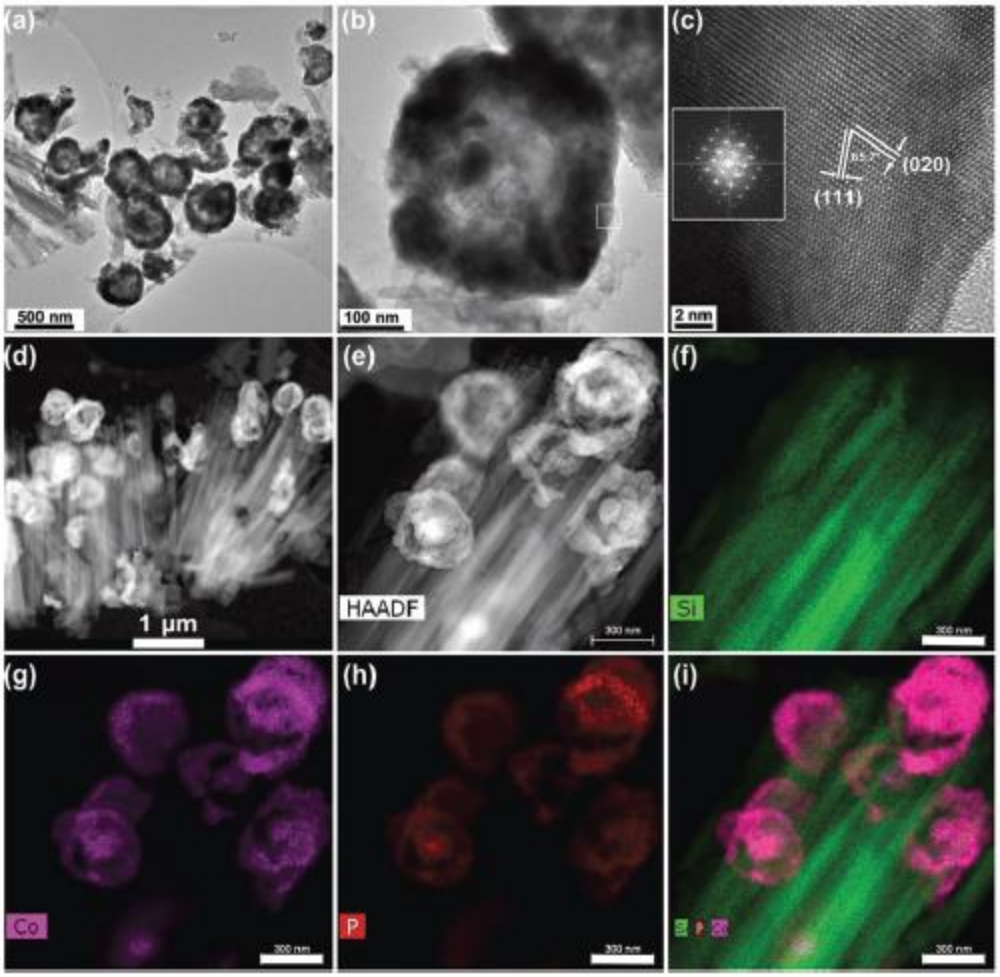

Fig 3 - (a, b) TEM and (c) high-resolution TEM images of Co_2P hollow spheres. Inset: ED pattern. (d, e) HAADF-STEM micrographs showing the morphology of the SiNW/Co-P-500 hybrids. Elemental maps of (f) Si, (g) Co and (h) P. (i) The overlap elemental map. Scale bars: 300 nm.

The PEC performance of the fabricated SiNW/Co-P electrodes were evaluated by linear scan voltammetry (LSV) and electrochemical impedance spectroscopy (EIS) in 0.5 M K_2SO_4 solution buffered at pH = 1. Fig. 4a shows the polarization (J–U) curves measured in the dark and under illumination for the SiNW/Co-P- 400, -500, and -600 electrodes having a Co-P catalyst loading of ca. 17.1, 17.7, and 18.3 µg cm^{-2},

respectively. For comparison, the J–U curves of bare SiNW and SiNW/PtNPs arrays are also presented as a reference. A lower catalyst loading of ca. 3.9 μg cm^{-2} was obtained for the SiNW/PtNPs since the NWs are short in length and the electroless deposition only enables a low coverage of PtNPs on SiNW arrays.[8] As shown in Fig. 4a, all the electrodes show extremely low cathodic current in the dark. Under illumination, the HER Vonset of the bare SiNW arrays is -0.16 V vs. RHE, and there is only negligible photocurrent generated at 0 V vs. RHE (ca. 0.2mA cm^{-2}), consistent with the previous report on the SiNW photocathodes fabricated by the same method, i.e., MACE.[6b] In contrast, the SiNW/ Co-P-400, -500, and -600 electrodes show remarkable positively shifted Vonset, amounting to 0.26, 0.21, and 0.34 V vs. RHE, respectively (Fig. S4, ESI†). Moreover, the photocurrent densities of these electrodes reach 10.8, 18.2, and 15.6mA cm^{-2} at 0 V, which are 54, 91, and 78 times, respectively, higher than that of the bare SiNW arrays. The fill factor of the SiNW/Co-P electrodes is relatively low, which presumably reflects a shunt resistance.[5b] Nevertheless, the overall PEC performance of the SiNW/Co-P photocathodes is found to be comparable to that of most PtNP decorated SiMW/ SiNW arrays reported in the literature (Table S1, ESI†).

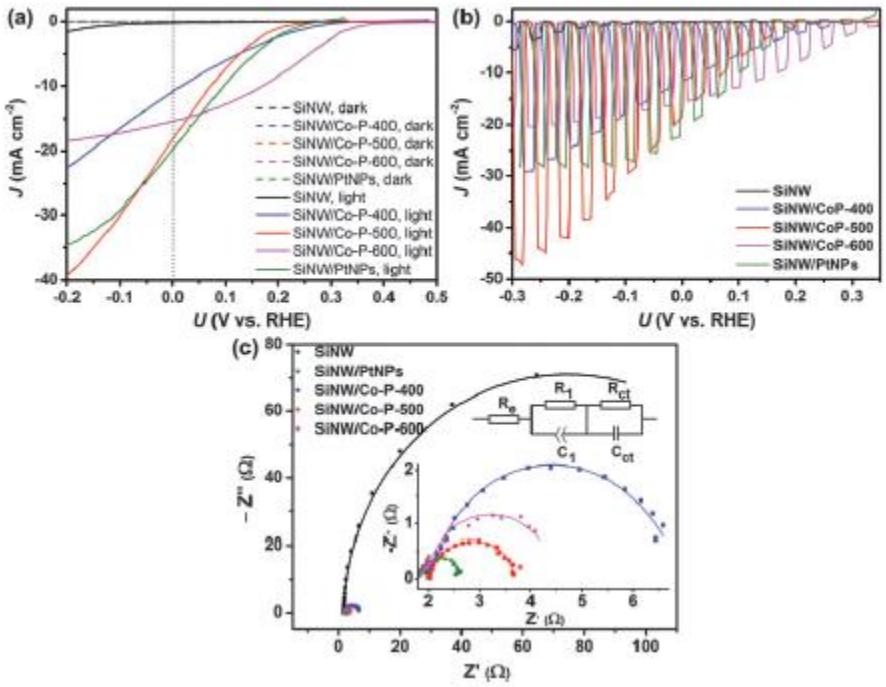

Fig 4- (a) J–U profiles of the SiNW, SiNW/PtNPs, SiNW/Co-P-400, -500, and -600 electrodes recorded in 0.5 M K_2SO_4 (pH = 1) under nominal illumination of 100 mW cm^{-2} (actually light intensity: 60 mW cm^{-2}, ESI†). Scan rate: 20 mV s^{-1}. (b) J–U profiles of the electrodes recorded under chopped illumination with a frequency of 0.5 Hz. Scan rate: 20 mV s^{-1}. (c) Nyquist plots of the electrodes recorded at 0 V vs. RHE under illumination. Inset: zoomed view of the plots from the SiNW/PtNPs and SiNW/Co-P electrodes; the equivalent circuit model used to fit experimental data.

It is believed that the remarkable enhancement in PEC performance of the SiNW/Co-P cathodes primarily originates from the excellent electrocatalytic properties of the Co-P catalysts. To clarify this, a bare SiNW array was directly phosphorized under the same conditions used for SiNW/Co-P-500 or SiNW/Co-P-600 preparation (i.e., 500 or 600 ^{o}C, 6 h, denoted as SiNW-500 and SiNW-600, respectively). It is found that the phosphorization treatment indeed positively shifts Vonset by ca. 0.11 and 0.16 V for SiNW-500 and SiNW-600 (Fig. S5, ESI†), and therefore improves the photocurrent densities at 0 V from the original -0.2 to -0.5 and -1.1 mA cm^{-2}, respectively, due probably to the formation of a thin P-doped Si layer (n^{-}-Si) on the surface of the p-SiNWs. However, this cannot account for the large improvement in the Vonset (Fig. S4, ESI†) and the photocurrent density increase observed from the SiNW/Co-P cathodes. Furthermore, we can rule out the possibility of enhanced light absorption resulting from the introduction of Co-P spheres, because the UV-Vis spectra show that after coupling with the Co-P spheres, the light absorption of the SiNW arrays actually decreases (Fig. S6, ESI†). Therefore, the excellent electrocatalytic performance of the Co-P hollow spheres must play a dominant role in the enhancement of PEC H_2 evolution. This is actually also corroborated by the J–U curves measured in the dark that unambiguously show that the Co-P spheres are electrocatalytically active (Fig. S7, ESI†).

Fig. 4b exhibits the photocurrent transient curves measured under chopped illumination at a frequency of 0.5 Hz. All the SiNW/Co-P electrodes start to show photo-response in between 0.15 and 0.35 V vs. RHE, while no obvious photo-response can be seen from the bare SiNW arrays unless the potential is more negative than - 0.1 V. Moreover, for all the electrodes, no current spikes are observed upon turning the light on/off, indicating that no significant surface recombination took place during the test. Fig. 4c shows the Nyquist plots of the SiNW, SiNW/PtNPs, SiNW/Co-P-400, -500 and -600 electrodes that were recorded at 0 V under illumination in the range of 105–0.1 Hz and fitted by a Randle model (for SiNW) and the equivalent circuit shown in the inset of Fig. 4c (for SiNW/PtNPs and SiNW/ Co-P electrodes). According to the fitting results (Table S2, ESI†), the equivalent series resistance (Re), including the contributions from the electrode material, electrical contact and electrolyte, of the bare SiNW array is 1.66 Ω. After decorating the SiNW array with the Co-P spheres, the Re only slightly increases, indicating that the Co-P catalysts have reasonably good conductivity. Moreover, the charge transfer resistance (Rct) of the SiNW/Co-P electrodes biased at 0

V, being 3.42, 1.02, and 1.52 Ω for SiNW/Co-P-400, -500, and -600, respectively, is found to be comparable to that of SiNW/PtNPs (i.e., 0.73 Ω) and is significantly smaller than that of the bare SiNW array (i.e., 145.40 Ω). This suggests that the hollow Co-P spheres greatly accelerate the charge transfer kinetics during the HER.

Fig. 5 shows preliminary results of the operation stability (J–t) test of the selected SiNW/Co-P-500 and -600 electrodes versus the SiNW/PtNPs. The test was performed in 0.5 M K_2SO_4 solution (pH = 1) at 0.1 V vs. RHE under a nominal illumination of 100mWcm^{-2} (with an actual light intensity of 60mWcm^{-2}, Fig. S9, ESI†). Initially, the photocurrent density of the SiNW/PtNPs is higher than that of SiNW/Co-P-500, but it decreases rapidly and becomes smaller after ≈700 s. After 2000 s, the photocurrent density of the SiNW/PtNPs electrode reduces by 60.0%; in contrast, that of the SiNW/Co-P-500 and -600 only decreases by 14.7% and 20.0%, respectively, in the same time-interval. SEM and EDX analyses indicate that the O content of the tested SiNW/PtNPs electrode is dramatically increased and the density of PtNPs becomes low after the J–t test (Fig. S8, ESI†). This suggests that gradual oxidation of SiNWs and partial loss of PtNPs lead to the fast degradation of the SiNW/PtNPs electrode. Given that the side walls of the SiNWs are not protected, progressive oxidation also occurs for the SiNW/Co-P-500 and -600 electrodes, resulting in a decrease in photocurrent density. The SiNW/PtNPs, SiNW/Co-P-500 and -600 electrodes lasted for ca. 2260, 2500, and 3160 s, respectively, before they eventually failed. The abrupt decrease in photocurrent density at the end of their lifetime likely arises from the increasing thickness of the SiO_x layer that reaches a threshold beyond which the electron transport is blocked. It is believed that the SiNW/Co-P electrode would be able to last for a much longer period of time if the side walls of SiNWs could be appropriately passivated[9] or the surface of SiNWs would be uniformly and conformally covered with the acid-stable Co-P catalysts. Further improvement in the electrode stability is under investigation.

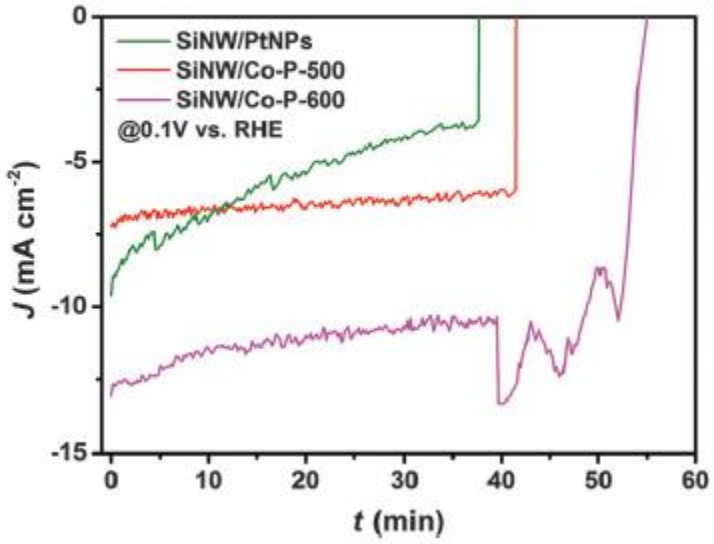

Fig 5 - J–t profiles of the SiNW/Co-P-500, SiNW/Co-P-600, and SiNW/ PtNPs electrodes recorded in 0.5 M K_2SO_4 solution (pH = 1) at 0.1 V vs. RHE under nominal illumination of 100 mW cm^{-2}.

In summary, we report the first example of SiNW array photocathodes coupled with hollow spheres of the emerging earth-abundant cobalt phosphide co-catalysts, which were fabricated through photo-assisted electrodeposition of cobalt on the SiNW surface, followed by a phosphorization treatment. The SiNW/Co-P photocathodes exhibit remarkable positively shifted onset potential and greatly enhanced photocurrent density toward solar-driven H_2 evolution, compared to the performance of SiNW arrays decorated with benchmark PtNPs. The improved performance originates from the excellent catalytic properties of cobalt phosphide spheres exhibiting very small charge transfer resistance. Compared with other non-precious catalysts being investigated such as MoS_2,[10] Mo_2C,[11] and WS_2,[12] the constitutional elements of cobalt phosphide are more earth-abundant, and therefore the cobalt phosphide decorated SiNW arrays hold substantial promise for use as low-cost photocathodes in water splitting cells.

L. F. Liu acknowledges the financial support by the FCT Investigator grant (IF/01595/2014).

Notes and references

1 R. N. Dominey, N. S. Lewis, J. A. Bruce, D. C. Bookblader and M. S. Wrighton, J. Am. Chem. Soc., 1982, 104, 467–482.

2 J. Zhu, Z. F. Yu, G. F. Burkhard, C. M. Hsu, S. T. Connor, Y. Q. Xu, Q.Wang,M. McGehee, S.H. Fan and Y. Cui, Nano Lett., 2009, 9, 279–282.

3 E. C. Garnett, M. L. Brongersma, Y. Cui and M. D. McGehee, Annu. Rev. Mater. Res., 2011, 41, 269–295.

4 Y. D. Hou, B. L. Abrams, P. C. K. Vesborg, M. E. Bjorketun, K. Herbst, L. Bech, A. M. Setti, C. D. Damsgaard, T. Pedersen, O. Hansen, J. Rossmeisl, S. Dahl, J. K. Norskov and I. Chorkendorff, Nat. Mater., 2011, 10, 434–438.

5 (a) A. P. Goodey, S. M. Eichfeld, K. K. Lew, J. M. Redwing and T. E. Mallouk, J. Am. Chem. Soc., 2007, 129, 12344–12345**; (b)** J. R. Maiolo, B. M. Kayes, M. A. Filler, M. C. Putnam, M. D. Kelzenberg, H. A. Atwater and N. S. Lewis, J. Am. Chem. Soc., 2007, 129, 12346–12347.

6 (a) P. D. Tran, S. S. Pramana, V. S. Kale, M. Nguyen, S. Y. Chiam, S. K. Batabyal, L. H. Wong, J. Barber and J. Loo, Chem. – Eur. J., 2012, 18, 13994–13999**; (b)** I. Oh, J. H. Kye and S. Hwang, Nano Lett., 2012, 12, 298–302; **(c)** Z. P. Huang, C. F. Wang, L. Pan, F. Tian, X. X. Zhang and C. Zhang, Nano Energy, 2013, 2, 1337–1346**; (d)** L. F. Liu and X. Q. Bao, Mater. Lett., 2014, 125, 28–31**; (e)** X. Q. Bao, R. Ferreira, E. Paz, D. C. Leitao, A. Silva, S. Cardoso, P. P. Freitas and L. F. Liu, Nanoscale, 2014, 4, 2097–2101; **(f)** X. Wang, K. Q. Peng, X. J. Pan, X. Chen, Y. Yang, L. Li, X. M. Meng, W. J. Zhang and S. T. Lee, Angew. Chem., Int. Ed., 2011, 50, 9861–9865.

7 (a) J. Q. Tian, Q. Liu, A. M. Asiri and X. P. Sun, J. Am. Chem. Soc., 2014, 136, 7587–7590; **(b)** E. J. Popczun, C. G. Read, C. W. Roske, N. S. Lewis and R. E. Schaak, Angew. Chem., Int. Ed., 2014, 53, 5427–5430.

8 (a) K. Q. Peng, X. Wang, X. L. Wu and S. T. Lee, Nano Lett., 2009, 9, 3704–3709; **(b) P**. C. Dai, J. Xie, M. T. Mayer, X. G. Yang, J. H. Zhan and D. W. Wang, Angew. Chem., Int. Ed., 2013, 52, 11119–11123.

9 X. Q. Bao and L. F. Liu, J. Power Sources, 2014, 268, 677–682.

10 (a) Y. G. Li, H. L. Wang, L. M. Xie, Y. Y. Liang, G. S. Hong and H. J. Dai, J. Am. Chem. Soc., 2011, 133, 7296–7299; **(b)** M. A. Lukowski, A. S. Daniel, F. Meng, A. Forticaux, L. S. Li and S. Jin, J. Am. Chem. Soc., 2013, 135, 10274–10277.

11 (a) H. Vrubel and X. L. Hu, Angew. Chem., Int. Ed., 2012, 51, 12703–12706**; (b)** W. F. Chen, C. H. Wang, K. Sasaki, N. Marinkovic, W. Xu, J. T. Muckerman, Y. Zhu and R. R. Adzic, Energy Environ. Sci., 2013, 6, 943–951.

12 D. Voiry, H. Yamaguchi, J. W. Li, R. Silva, D. C. B. Alves, T. Fujita, M. W. Chen, T. Asefa, V. B. Shenoy, G. Eda and M. Chhowalla, Nat. Mater., 2013, 12, 850–855.